A study of $Al_{1-x}In_xN$ growth by reflection high-energy electron diffraction—incorporation of cation atoms during molecular-beam epitaxy

B. M. Shi, Z. Y. Wang, M. H. Xie,[a] and H. S. Wu
Department of Physics, The University of Hong Kong, Pokfulam Road, Hong Kong, China

(Received 27 December 2007; accepted 16 February 2008; published online 10 March 2008)

Molecular-beam epitaxy of $Al_{1-x}In_xN$ alloys with different indium (In) contents, x, were studied by *in situ* reflection high-energy electron diffraction (RHEED). Growth rates of the alloys were measured by the RHEED intensity oscillations for different source flux conditions, while the lattice parameters were derived from the diffraction patterns. It was found that under the excess nitrogen growth regime, incorporation of aluminum was complete whereas incorporation of In atoms was incomplete even at temperatures below 400 °C. © *2008 American Institute of Physics*.
[DOI: 10.1063/1.2894191]

$Al_{1-x}In_xN$ ternary alloys have direct band gaps that cover a wide spectral range from ultraviolet to infrared wavelengths,[1] which would thus have tremendous potentials in optoelectronic and photovoltaic applications. Comparing to other III-nitride alloys (e.g., AlGaN and InGaN), AlInN remains scarcely studied due to the difficulties associated with the large miscibility gap, which makes the alloy prone to phase separation.[2–5] On the other hand, alloys of $Al_{1-x}In_xN$ show different strain characteristics, from tensile to compressive, when deposited on GaN substrate. One may even grow an alloy that is lattice matched to GaN, so AlInN/GaN-based multiple quantum wells of and superlattices may be fabricated pseudomorphically on GaN for some specific applications such as Bragg mirrors.[6]

In this letter, we present a study of $Al_{1-x}In_xN$ growth by *in situ* reflection high-energy electron diffraction (RHEED) during deposition by molecular-beam epitaxy (MBE). Since the MBE process is dominated by kinetics, the problems associated with the thermal stability and solubility of the alloys may be circumvented. As a matter of fact, $Al_{1-x}In_xN$ alloys with the full composition range ($0 \leqslant x \leqslant 1$) have been reportedly grown by using the plasma-assisted MBE technique.[7,8] However, due to the large difference in vapor pressures between aluminum (Al) and indium (In) over AlInN, incorporation of the two elements during growth will show different temperatures and flux dependences, which causes complications in compositional control. Here, we utilize the RHEED to follow the growth characteristics of the alloys and to derive the incorporation coefficients of both Al and In. It is found that under the cation flux limited growth regime [i.e., excess nitrogen (N)], incorporation of In is incomplete even at temperatures below 400 °C.

The MBE system contained conventional effusion cells for gallium (Ga), In and Al sources, and a radio-frequency plasma unit for N.[9] The substrate was nominally flat 6*H*-SiC(0001), upon which a thick ($\geqslant$3000 Å) GaN buffer layer of the Ga polarity was firstly grown at $\geqslant$620 °C under excess Ga.[9] Having completed the buffer film growth, the sample was subjected to a brief annealing procedure at 600 °C until the initial pseudo-(1×1) surface reconstruction changed to (2×2), characteristic of a clean surface without excess Ga adlayer on surface.[10] Afterward, the sample temperature was lowered to below 400 °C before commencing $Al_{1-x}In_xN$ deposition under various source flux conditions. The reason of choosing such low substrate temperatures ($\leqslant$400 °C) is to enhance In incorporation and maintain the layer-by-layer growth mode even for binary InN growth on GaN.[11] The fluxes of the metals and N were calibrated beforehand by the RHEED oscillations during InN, GaN, and AlN depositions in the N-rich and metal-rich regimes, respectively.[9,11] The RHEED was operated at 10 keV and the diffraction patterns and the specular beam intensity oscillations were recorded by a charge coupled device camera that was interfaced to a computer.

Figure 1 shows typical RHEED specular beam intensity oscillations during AlInN deposition, while the insets show the corresponding RHEED patterns taken along the $[11\bar{2}0]$ direction from (a) the starting GaN(0001)-(2×2) and (b) finishing AlInN surfaces. For the latter, only the (1×1) pattern was observed. The persistent RHEED intensity oscillations as well as the streaky RHEED patterns suggest the layer-by-layer growth mode of the alloy. From the oscillation frequency, we derive the deposition rate, where one oscillation period corresponds to one bilayer [BL, i.e., a layer of

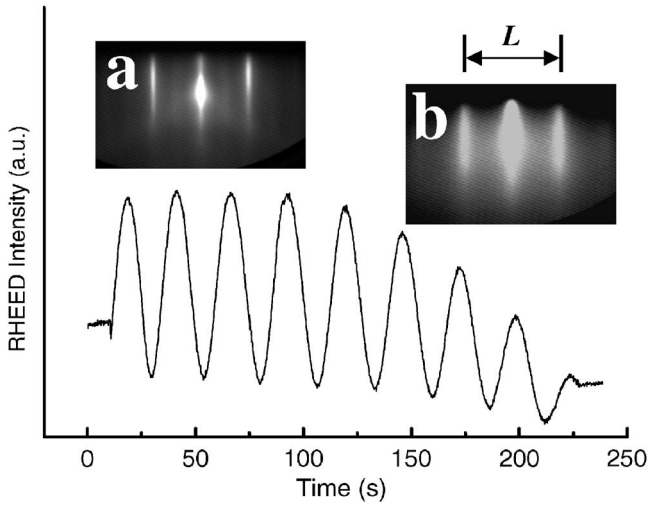

FIG. 1. RHEED specular beam intensity oscillations during AlInN deposition. Insets: the RHEED patterns taken along the $[11\bar{2}0]$ azimuth from (a) the starting GaN and (b) finishing AlInN surfaces, respectively.

[a]Author to whom correspondence should be addressed. Electronic mail: mhxie@hkusua.hku.hk.

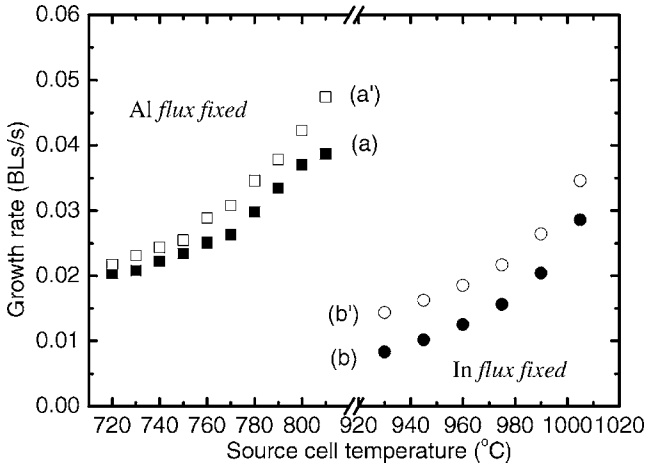

FIG. 2. Growth rate of AlInN as derived from the RHEED oscillations (solid symbols) for growth under a fixed Al flux of 0.017 BLs/s but varying In fluxes (a), and under a fixed In flux of 0.01 BLs/s but varying Al fluxes (b). The open symbols represent the expected growth rate from the source fluxes (a' and b'), assuming complete atom incorporation.

anion (N) plus a layer of cation (In and/or Al) atoms along the [0001] direction] material growth.[9,12] Figure 2 presents the derived AlInN growth rates under (a) a fixed Al but varying In source temperature and (b) under a fixed In but varying Al cell temperature. The figure also plots the "expected" rates from the source fluxes at the given source cell temperatures, assuming complete incorporation of the depositing atoms. By comparing the measured rates of the alloy growth with the "expect" ones, we observe clear deviations. The alloys grow at slower rates than expected, which implies incomplete incorporation of In and/or Al atoms in the alloys.

To investigate the incorporation behavior of Al and In, we plot in Fig. 3 the alloy growth rates as functions of (a) Al and (b) In fluxes. Let α_{Al} and α_{In} be the incorporation coefficients of Al and In, respectively, one may express AlInN growth rate as $R_{AlInN}=\alpha_{Al}R_{Al}+\alpha_{In}R_{In}$ in the regime of excess N. Here, R_{Al} and R_{In} denote the fluxes of Al and In, respectively, as derived from the growth rates of AlN and InN, respectively. By linear fitting of the data, one may derive the coefficients α_{Al} and α_{In} from the slopes and intercepts of the lines. Such line fittings are shown in the figure by the solid lines and the derived incorporation coefficients are $\alpha_{Al}\approx 1.0$ and $\alpha_{In}\approx 0.77$ for Al and In, respectively. In other words, at the temperature of deposition ($\leqslant$400 °C), Al incorporation is complete whereas In incorporation is only about 77%.

An immediate question is where those unincorporated indium atoms go. At this stage, we do not have a definite answer yet, but we speculate that they are either desorbed from the growing surface or, if they stay on surface, they form In wetting layers and/or droplets. We do occasionally observe metallic droplets on surface, but we cannot be certain if they are solely of In or having other contributions as well. On the other hand, due to a relatively weak adsorption of In on AlInN, surface desorption of In atoms is also possible. Studies of temperature dependence of α_{Al} and α_{In} are underway, and the results will be included in future publications.

After completing the RHEED oscillations, we also measured the spacing L between the (01) and $(0\bar{1})$ diffraction streaks on the RHEED (refer to the inset of Fig. 1). By

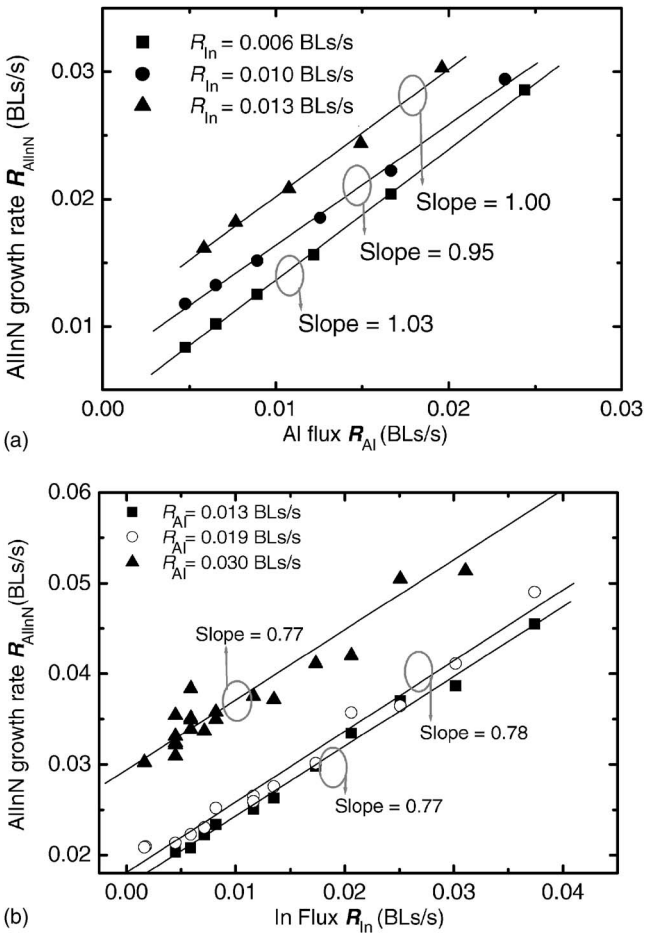

FIG. 3. AlInN growth rates as a function of (a) Al and (b) In fluxes, respectively. In each figure, three sets of data are shown corresponding to different, but fixed In (a) or Al (b) fluxes. The solid lines represent the least square fittings of the data with the resulted slopes marked.

comparing to L_{GaN} of the GaN substrate, we derive the lattice mismatch between the grown alloy and GaN according to $f=(a-a_{GaN})/a_{GaN}=(L_{GaN}-L)/L$, where a and a_{GaN} are the in-plane lattice parameters of the alloy and GaN, respectively. L and L_{GaN} are obviously the reciprocals of a and a_{GaN}. The results are plotted in Fig. 4 against the alloy

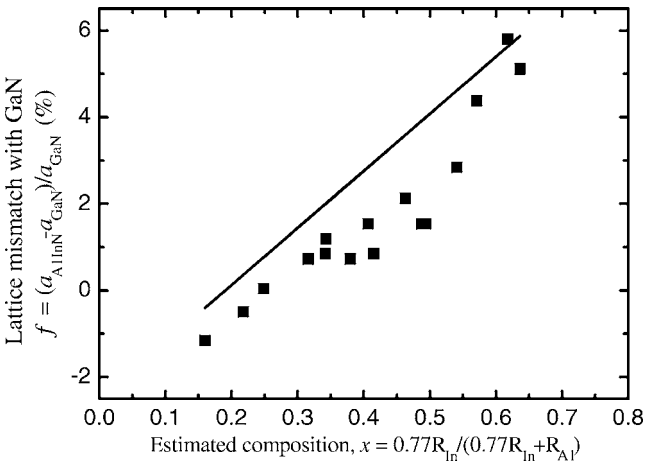

FIG. 4. In-plane lattice mismatch, f, of the epitaxial $Al_{1-x}In_xN$ on GaN(0001) plotted against the alloy composition, x. The solid line represents the ideal $f-x$ relation, assuming that Vegard's law is valid for the alloy's lattice constant and that the epifilm is strain-free.

compositions x estimated from the source fluxes, taking $\alpha_{Al}=1.0$ and $\alpha_{In}=0.77$. The solid line in figure represents the "ideal" lattice mismatch, assuming Vegard's law for the alloy's lattice constant (i.e., assuming $a_{Al_{1-x}In_xN}=(1-x)a_{AlN}+xa_{InN}$). From the figure, one observes the correct trend of the alloy's lattice constant with composition, suggesting that alloys of different compositions have been achieved by choosing the different combinations of the In and Al fluxes. On the other hand, we also observe deviations between the measured lattice parameter and the ideal value. Such deviations may be due to errors in estimating x from the source flux, or even more likely, due to the presence of residual strains in the epitaxial alloys. Indeed, incomplete relaxation of strain in the epifilm causes its in-plane lattice constant to be different from that of a strain-free alloy. Particularly, for thin films of alloys with small lattice misfits, the epilayers can grow coherently, taking the in-plane lattice parameter of the substrate.[13] Therefore, incomplete strain relaxation of the epilayer leads to an in-plane lattice parameter of the alloy being closer to that of the substrate. This seems to be consistent with the fact that the data points in Fig. 4 are below the ideal line. There is, however, another possible reason for the observed deviation, which is related to that the RHEED actually measures the lattice parameter of the near surface layer. The latter can be different from the lattice of the bulk. Not only the lattice may be more relaxed near the surface but also that the composition of the alloy near surface can be different from that of the bulk due to, e.g., the effect of surface segregation.[14] The latter effect, however, remains to be studied for the AlInN system. Because of all such complications, we shall not comment further on the detailed features of Fig. 4 (such as the seemingly nonlinearity of the $f\sim x$ relation).

Finally, we note in passing that as the deposited alloy layers are likely partially strained, the strain state may also affect the incorporation kinetics of the cation atoms. From the results of Fig. 3, however, we remark that such an effect is not so obvious for AlInN alloy growth. Indeed, when the fluxes of In and/or Al vary, the composition of the deposited alloy also changes. The latter may then cause different residual strains in the alloy layers. If the incorporation of Al and In were affected by the strain, nonlinear relations between R_{AlInN} and $\alpha_{In,Al}$ could be expected. The slopes of the three lines in Figs. 3(a) and 3(b) would also be different. The experiments of Fig. 3 show just the opposite, implying either that the strain state are similar for all the alloys deposited or the incorporation coefficients α_{In} and α_{Al} are strain insensitive.

To summarize, strong RHEED intensity oscillations during AlInN growth are recorded. Together with the streaky RHEED patterns, the layer-by-layer growth mode of the alloys are suggested. From the RHEED oscillation frequencies or the growth rates, we derive the incorporation coefficients of the cation atoms. While Al incorporation is complete, In incorporation amounts to only about 77% at temperatures below 400 °C. On the other hand, having known the incorporation rates of Al and In, alloys of arbitrary composition may be grown by properly choosing the source flux combination.

This work was supported by a grant from the Research Grant Council of the Hong Kong Special Administrative Region, China, under the Grant No. HKU7055/06P.

[1] A. Trampert, O. Brandt, and K. H. Ploog, in *Gallium Nitrides I*, Semiconductor and Semimetals Vol. 50, edited by J. I. Pankove and T. D. Moustakas (Academic, New York, 1998), Chap. 7.
[2] T. Matsuoka, Appl. Phys. Lett. **71**, 105 (1997).
[3] J. Adhikari and D. A. Kofke, J. Appl. Phys. **95**, 6129 (2004).
[4] T. Takayama, M. Yuri, K. Itoh, T. Baba, and J. S. Harris, Jr., Jpn. J. Appl. Phys., Part 1 **39**, 5057 (2000).
[5] M. Ferhat and F. Bechstedt, Phys. Rev. B **65**, 075213 (2002).
[6] J.-F. Carlin and M. Ilegems, Appl. Phys. Lett. **83**, 668 (2003).
[7] M. J. Lukitsch, Y. V. Danylyuk, V. M. Naik, C. Huang, G. W. Auner, L. Rimai, and R. Naik, Appl. Phys. Lett. **79**, 632 (2001).
[8] W. Terashima, S. Che, Y. Ishitani, and A. Yoshikawa, Jpn. J. Appl. Phys., Part 2 **45**, L539 (2006).
[9] S. M. Seutter, M. H. Xie, W. K. Zhu, L. X. Zheng, H. Wu, and S. Y. Tong, Surf. Sci. **445**, L71 (2000).
[10] A. R. Smith, R. M. Feenstra, D. W. Greve, M.-S. Shin, M. Skowronski, J. Neugebauer, and J. E. Northrup, J. Vac. Sci. Technol. B **16**, 2242 (1998).
[11] Y. F. Ng, Y. G. Cao, M. H. Xie, X. L. Wang, and S. Y. Tong, Appl. Phys. Lett. **81**, 3960 (2002).
[12] J. H. Neave, P. J. Dobson, B. A. Joyce, and J. Zhang, Appl. Phys. Lett. **47**, 100 (1985).
[13] J. W. Matthews and A. E. Blakeslee, J. Cryst. Growth **27**, 118 (1974).
[14] J. J. Harris, D. E. Ashenford, C. T. Foxon, P. J. Dobson, and B. A. Joyce, Appl. Phys. A: Solids Surf. **33**, 87 (1984).